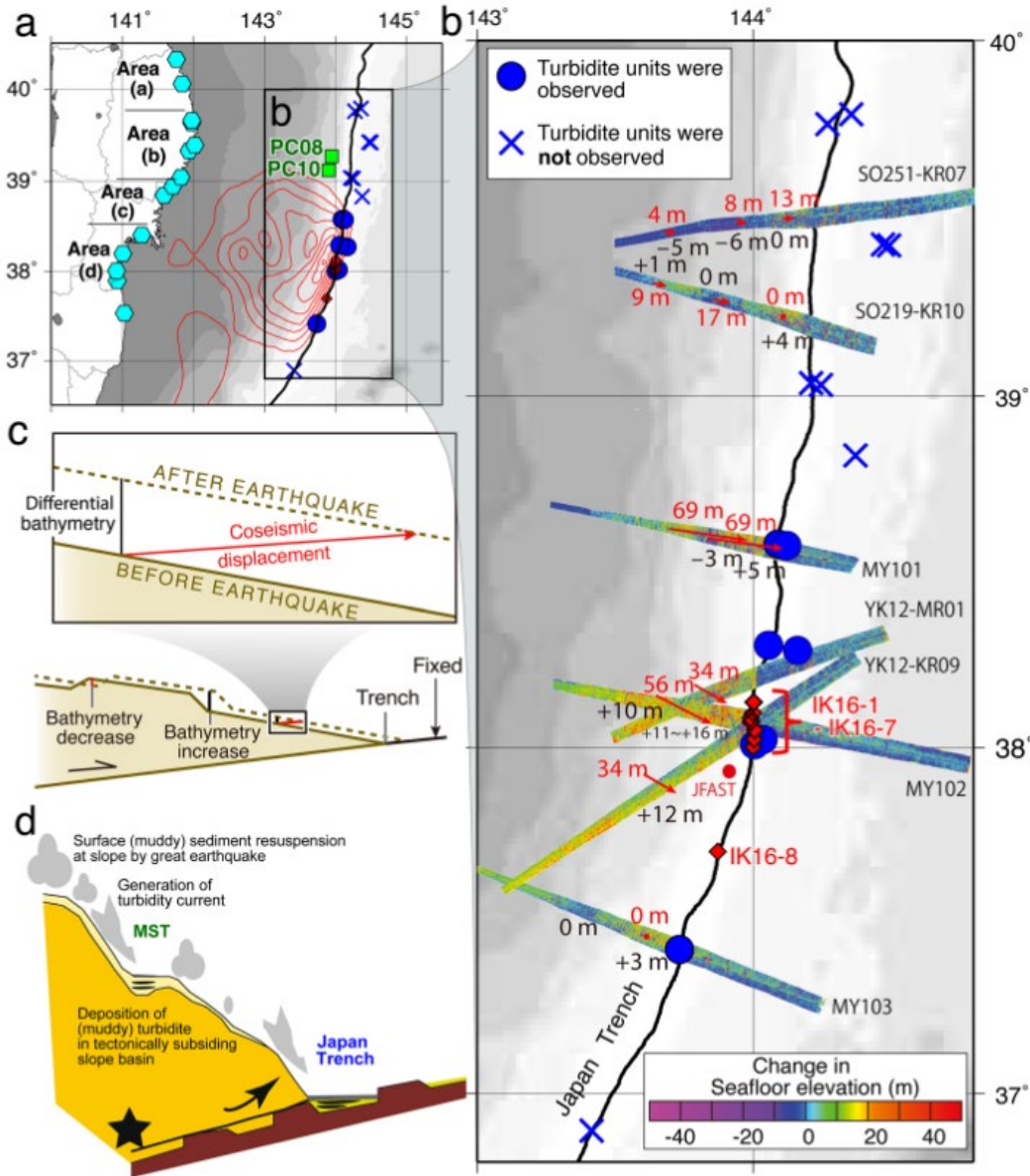


Dynamic viability of finite-fault slip models of the 2011 Mw 9.0 Tohoku-Oki earthquake and their role in tsunamigenic uplift

Jeremy Wing Ching Wong
 Alice-Agnes Gabriel
 Wenyuan Fan

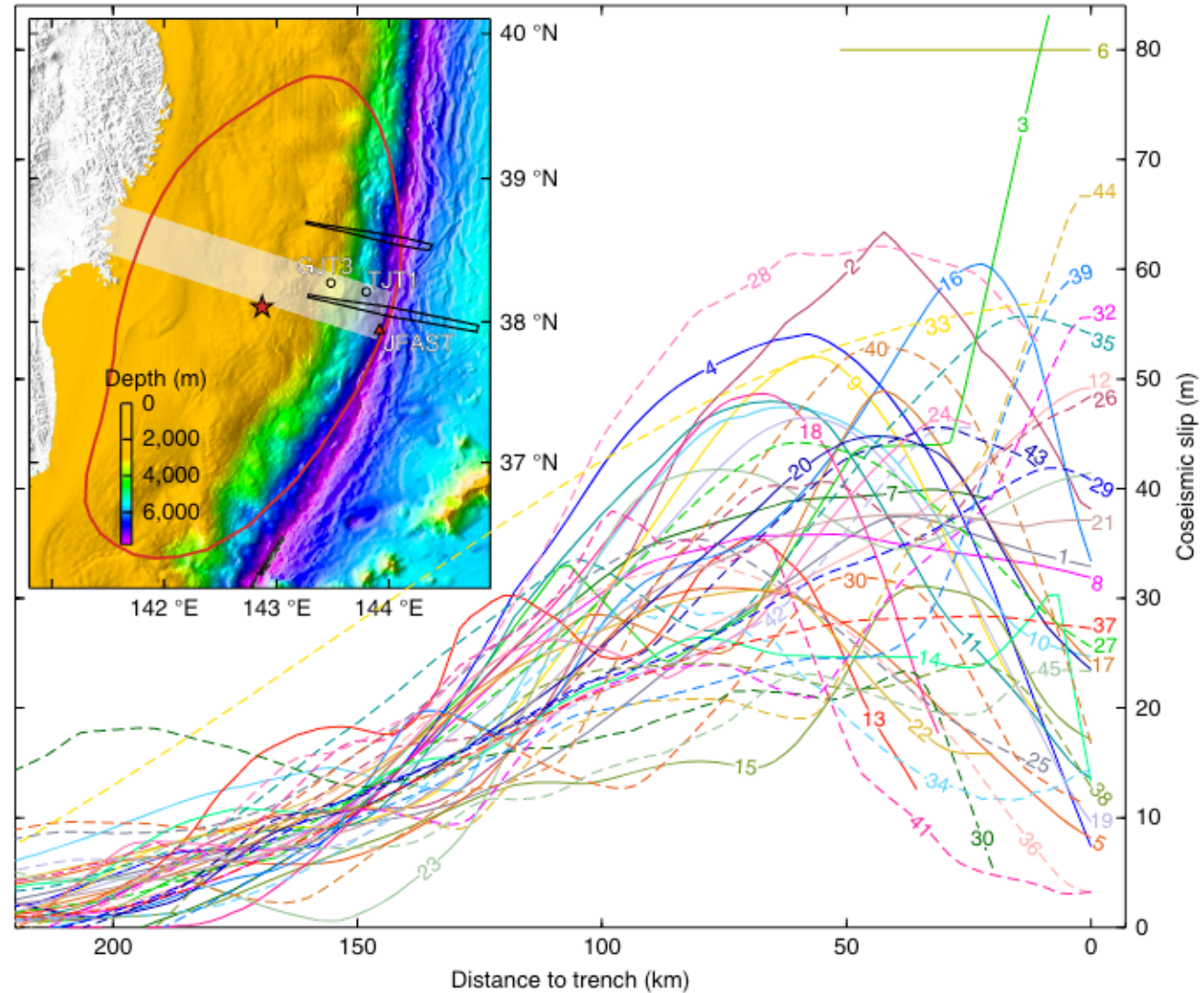
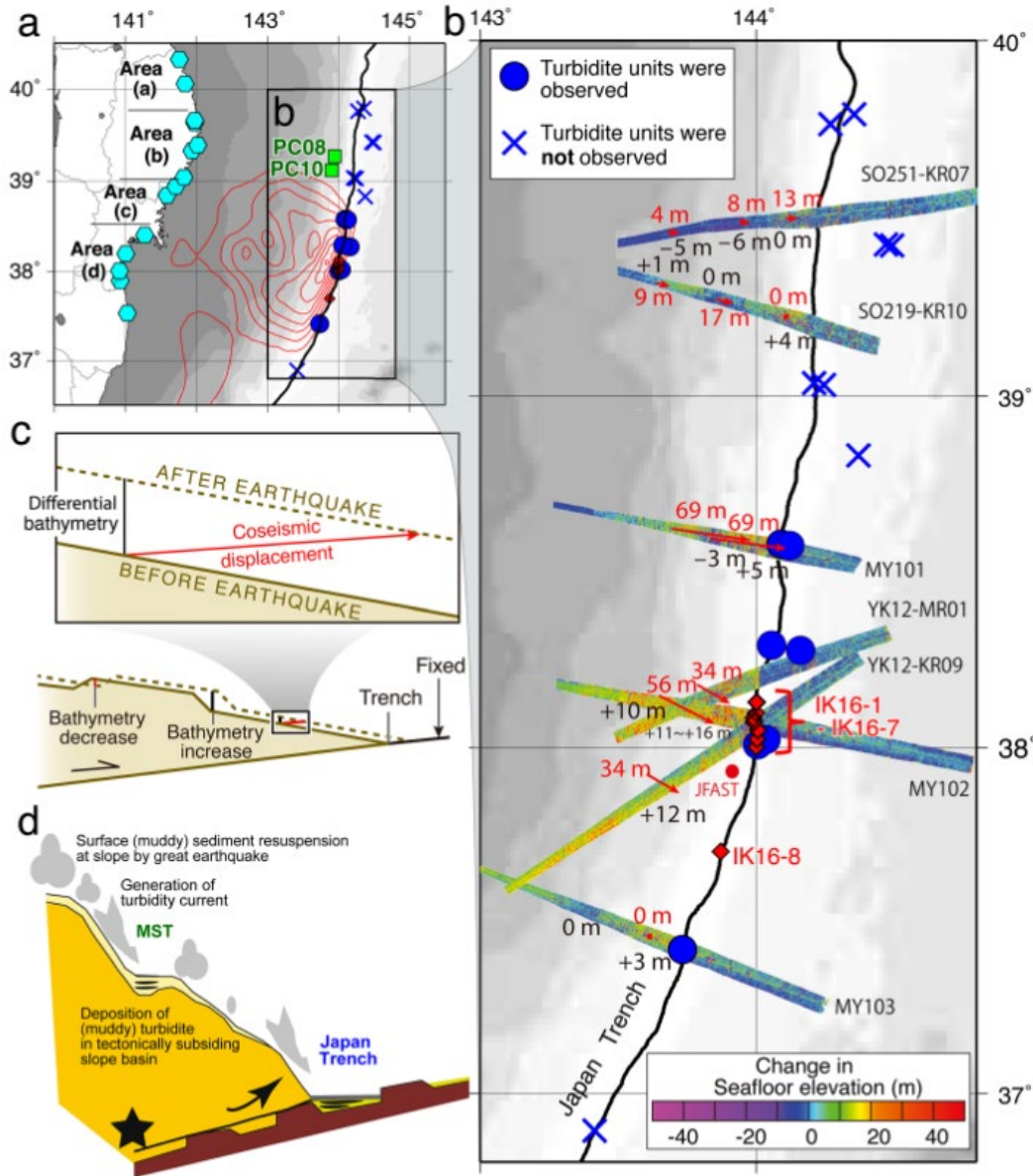


Unexpectedly large tsunami from the 2011 Mw 9.0 Tohoku-Oki earthquake

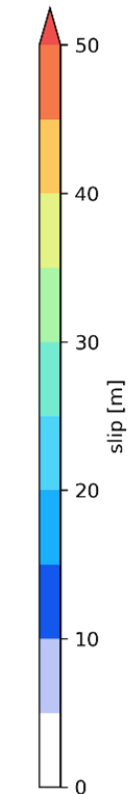
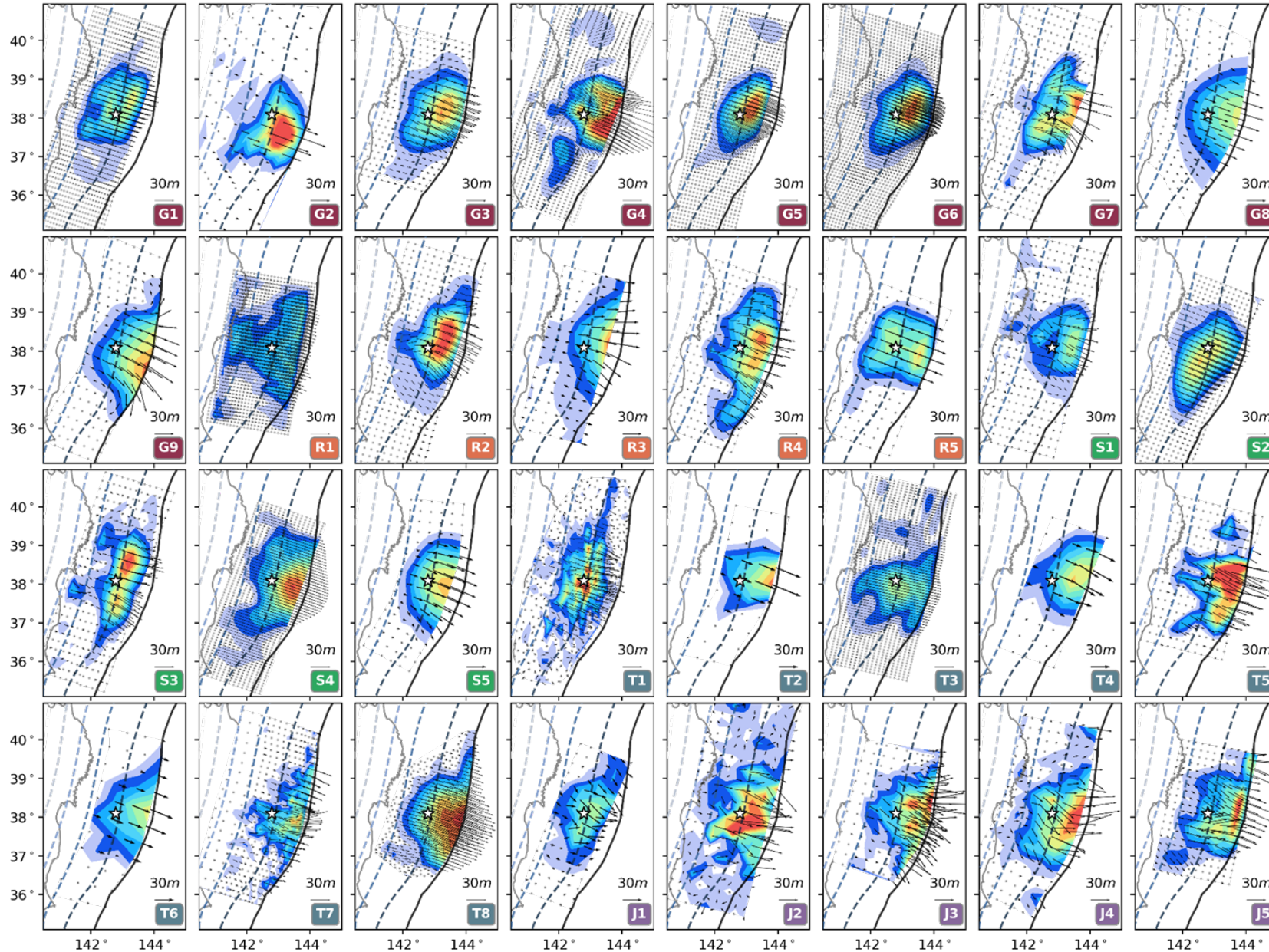


Tsunami of the 2011 Mw 9.0 Tohoku-Oki earthquake

Diverse near-trench slip estimates from finite-fault slip models



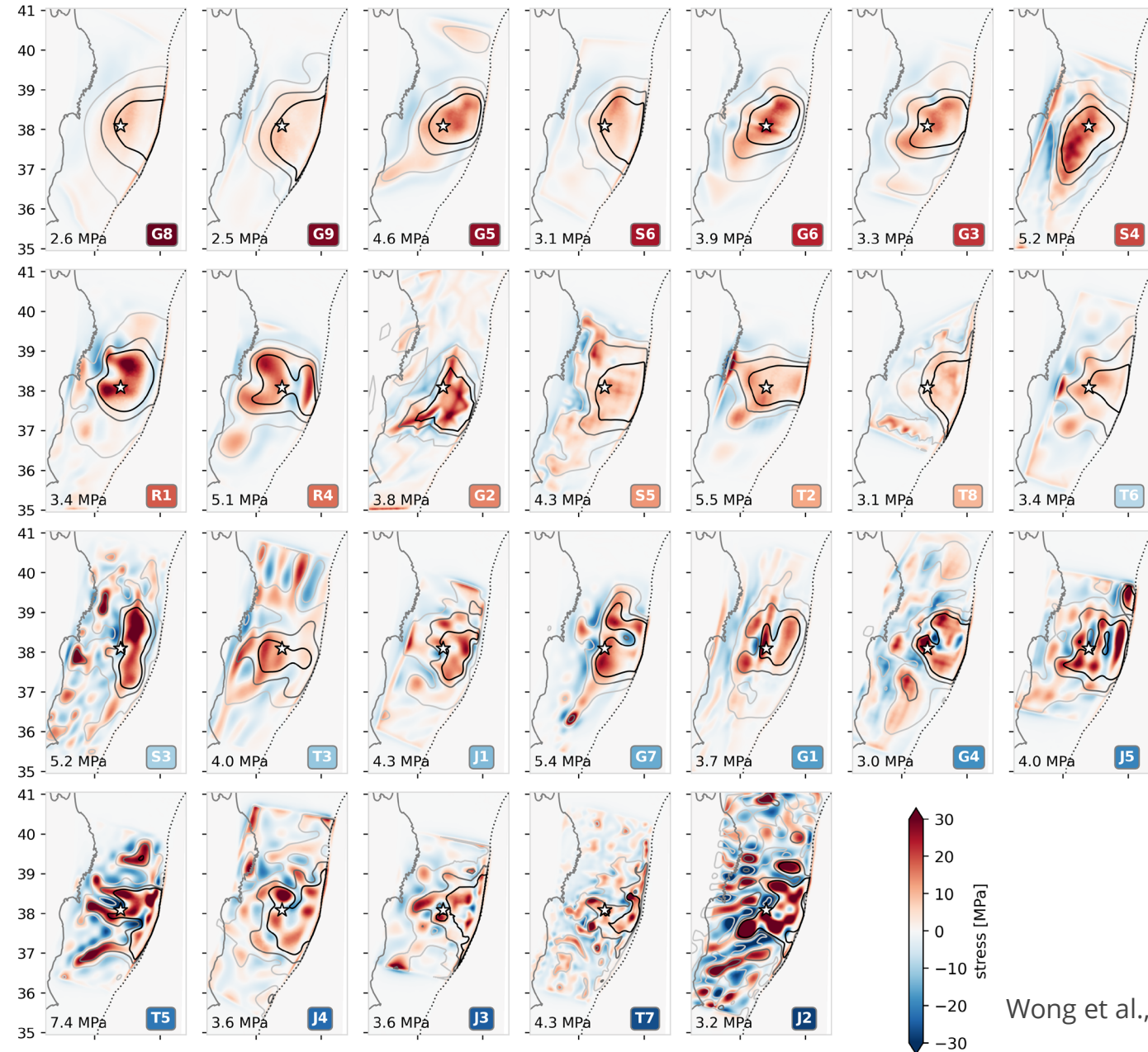
Large variability among published finite-fault slip models (FFMs)



- G** : Static geodetic
- R** : Regional seismic (and geodetic)
- S** : Teleseismic (and geodetic)
- T** : Tsunami (and geodetic)
- J** : Joint tsunami, seismic, and geodetic

- FFMs often used for comparison with kinematic coupling, afterslip models, seismicity, and structural observations
- Identify mechanically distinct fault regions, such as asperities and barriers

Diverse slip-derived stress-change patterns



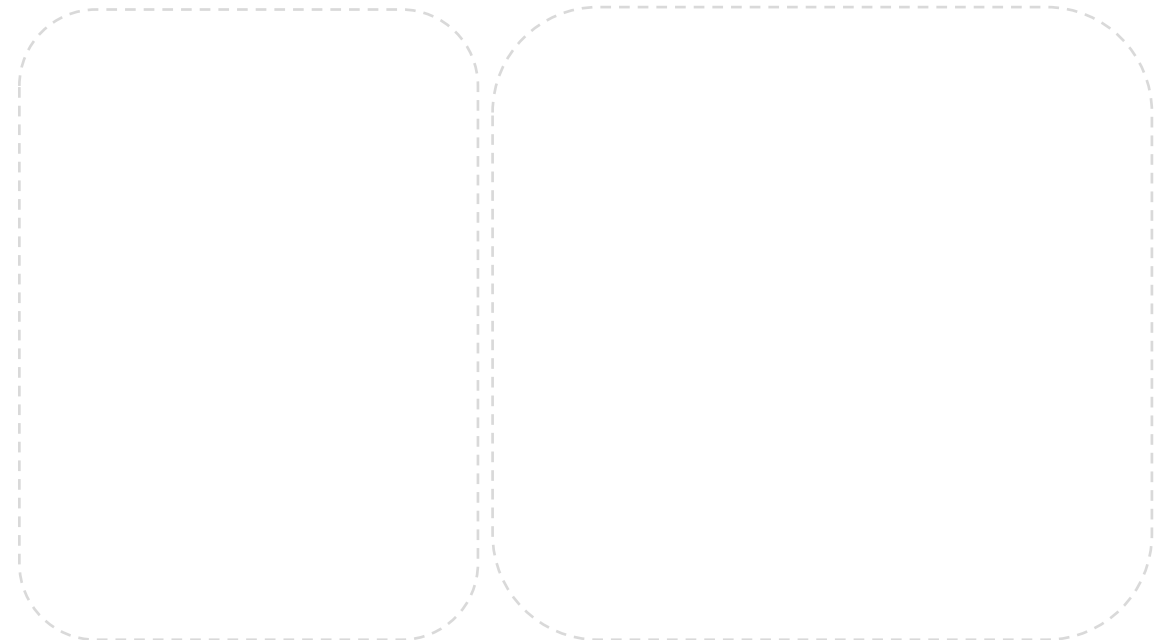
Increasing heterogeneity

- Heterogeneity may reflect variations in faulting conditions

Dynamic rupture simulations as **physics-based constraints** to evaluate dynamic viability of finite-fault slip models

- 3D Japan Integrated Velocity Structure Model (JIVSM)
- Fast velocity-weakening rate-and-state friction
- Off-fault plastic deformation
- Depth-dependent effective normal stress
($P_f = 0.9$ lithostatic stress)

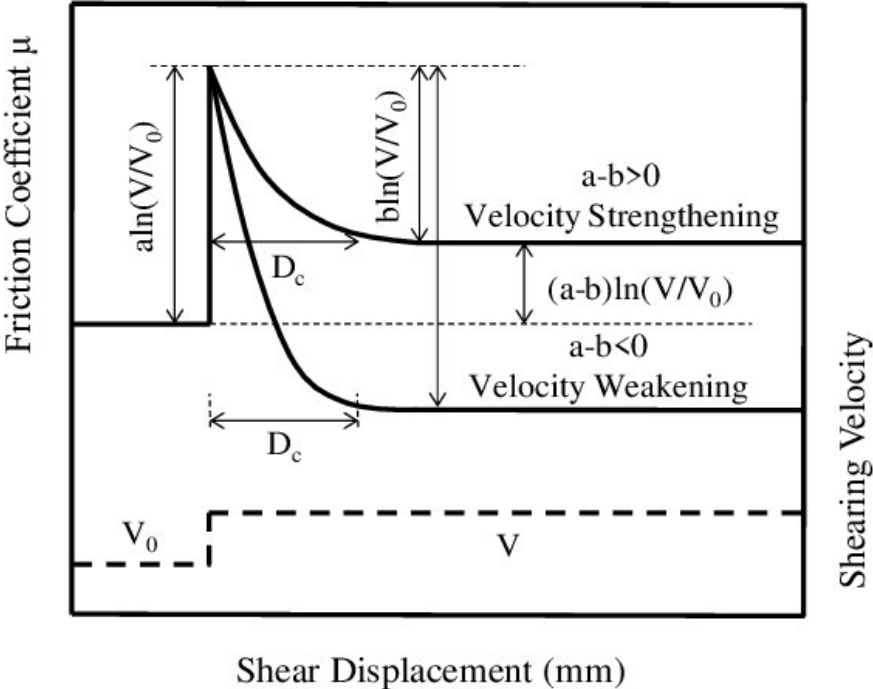
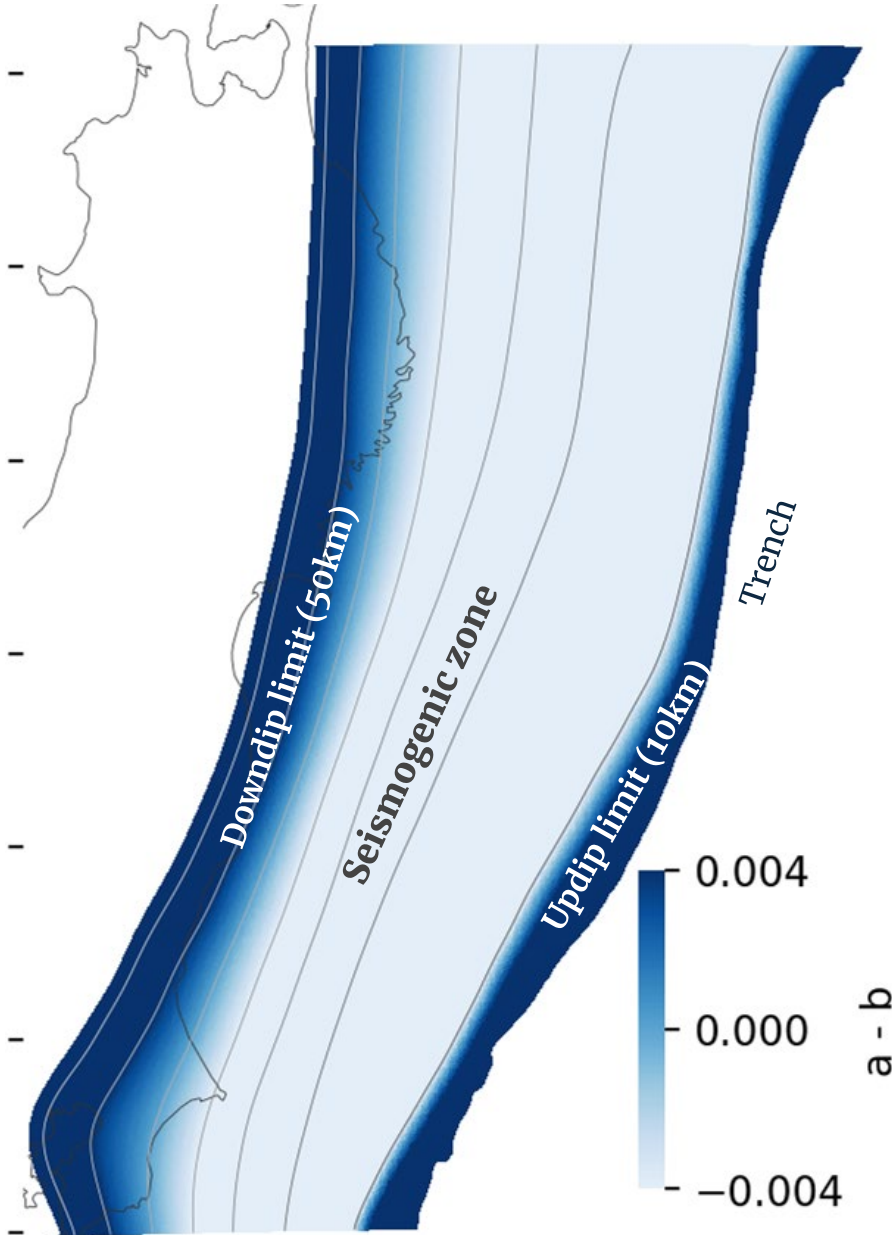
SeisSol



Friction: Fast velocity-weakening rate-and-state friction

At low slip rates ($\ll 0.1 \text{ m/s}$):

- Classical rate-and-state friction

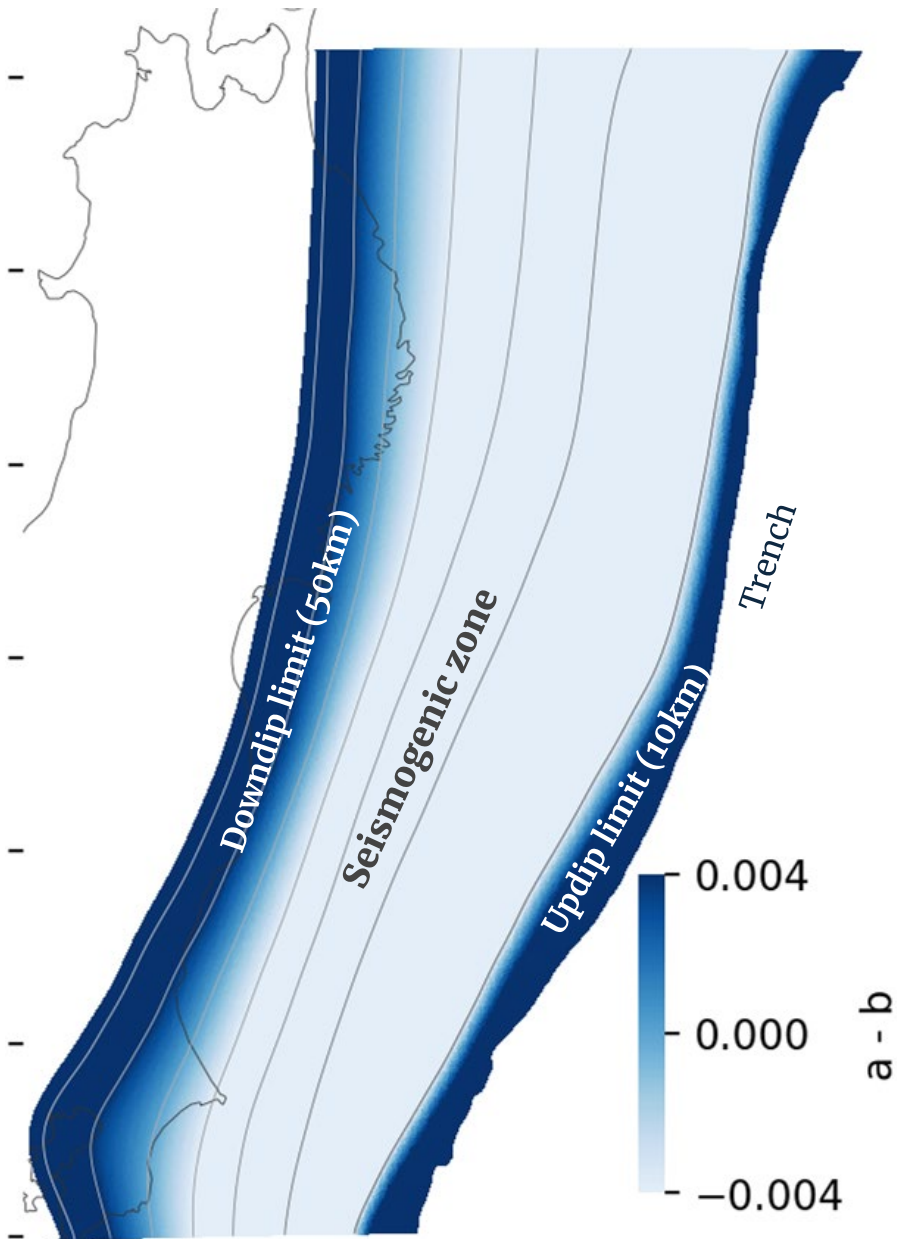


Seismogenic zone: velocity-weakening

Up-dip limit at 10 km, defined by the boundary between the accretionary wedge and crustal bedrock

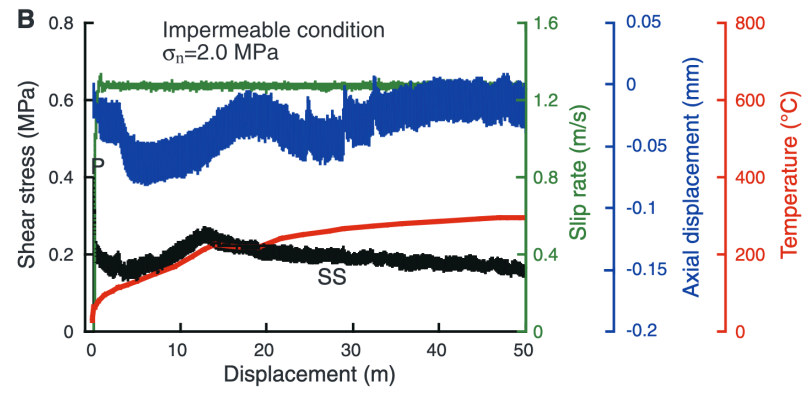
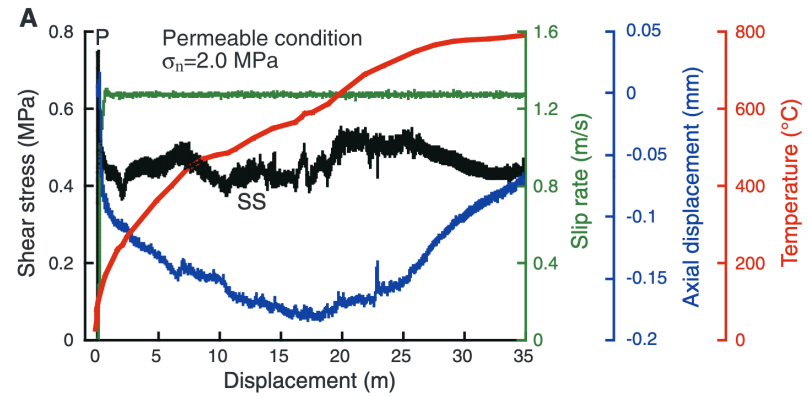
Down-dip limit at 50km, based on subduction zone seismicity

Friction: Fast velocity-weakening rate-and-state friction

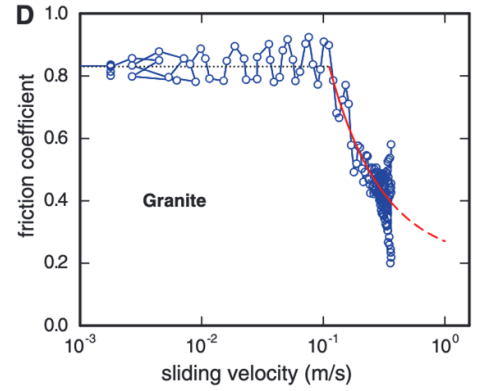
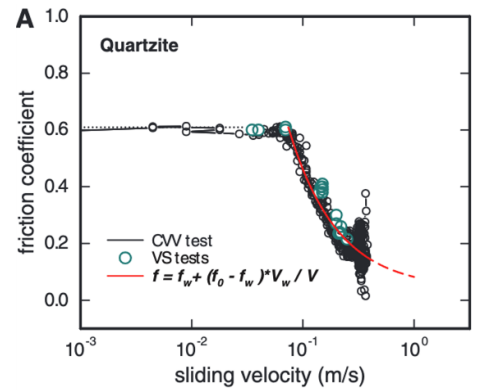


At high slip rates (~ 0.1 m/s):
$$f_{ss}(V) = f_w + \frac{f_{LV}(V) - f_w}{[1 + (V/V_w)^n]^{1/n}}$$

- Proxy for flash-heating & thermal pressurization which weaken friction at high slip rates ($V_w \geq 0.1$ m/s)



Ujiie et al., 2013



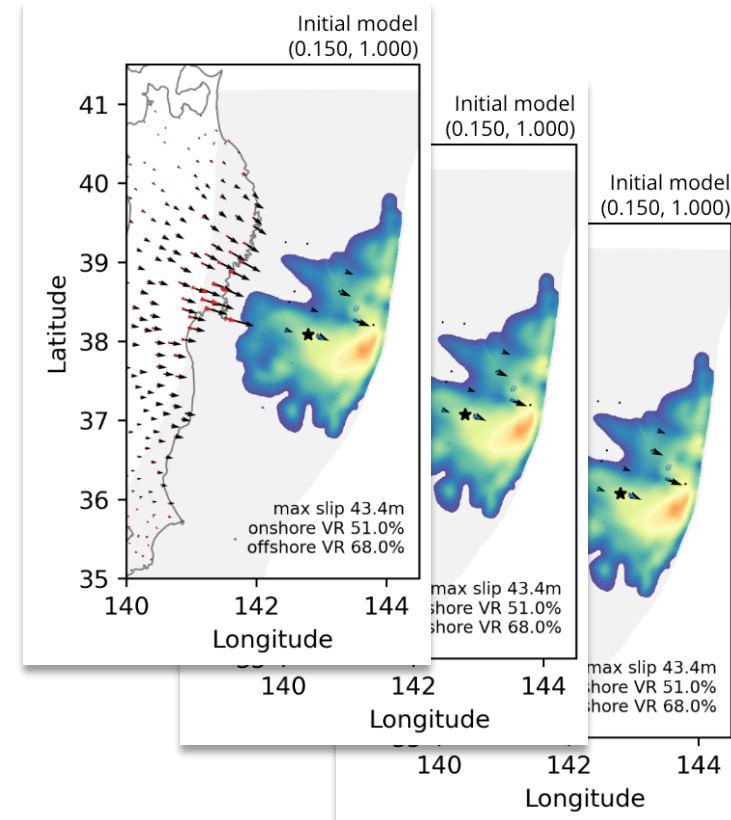
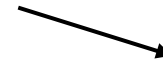
Goldsby and Tullis, 2011

Ensemble Kalman Inversion to identify best-fitting dynamic rupture scenarios

- run an ensemble of rupture simulations, sampling (α, R_0) for each FFMs derived prestress heterogeneity patterns

α

R_0

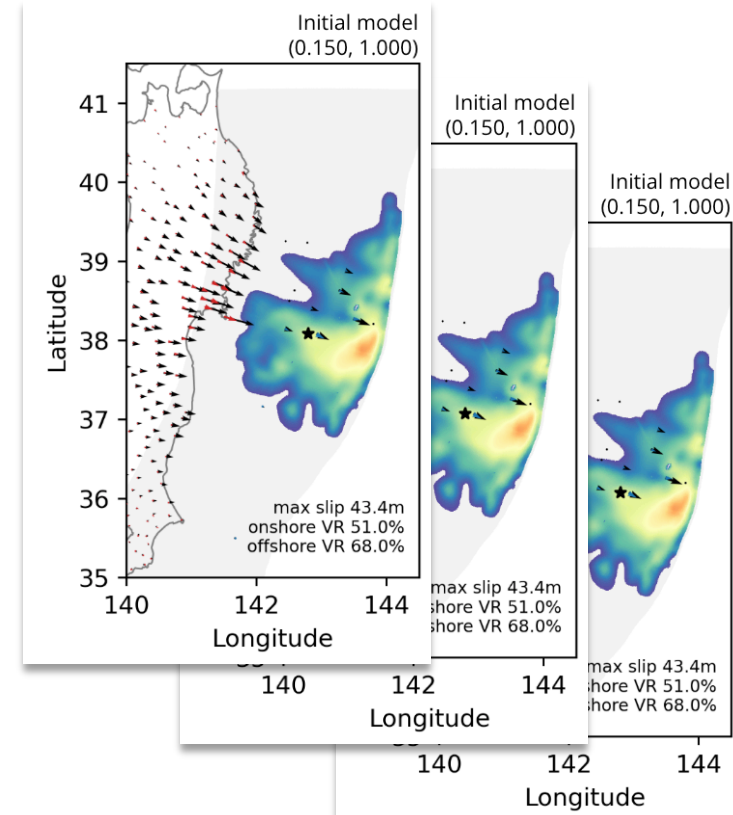


Ensemble Kalman Inversion to identify best-fitting dynamic rupture scenarios

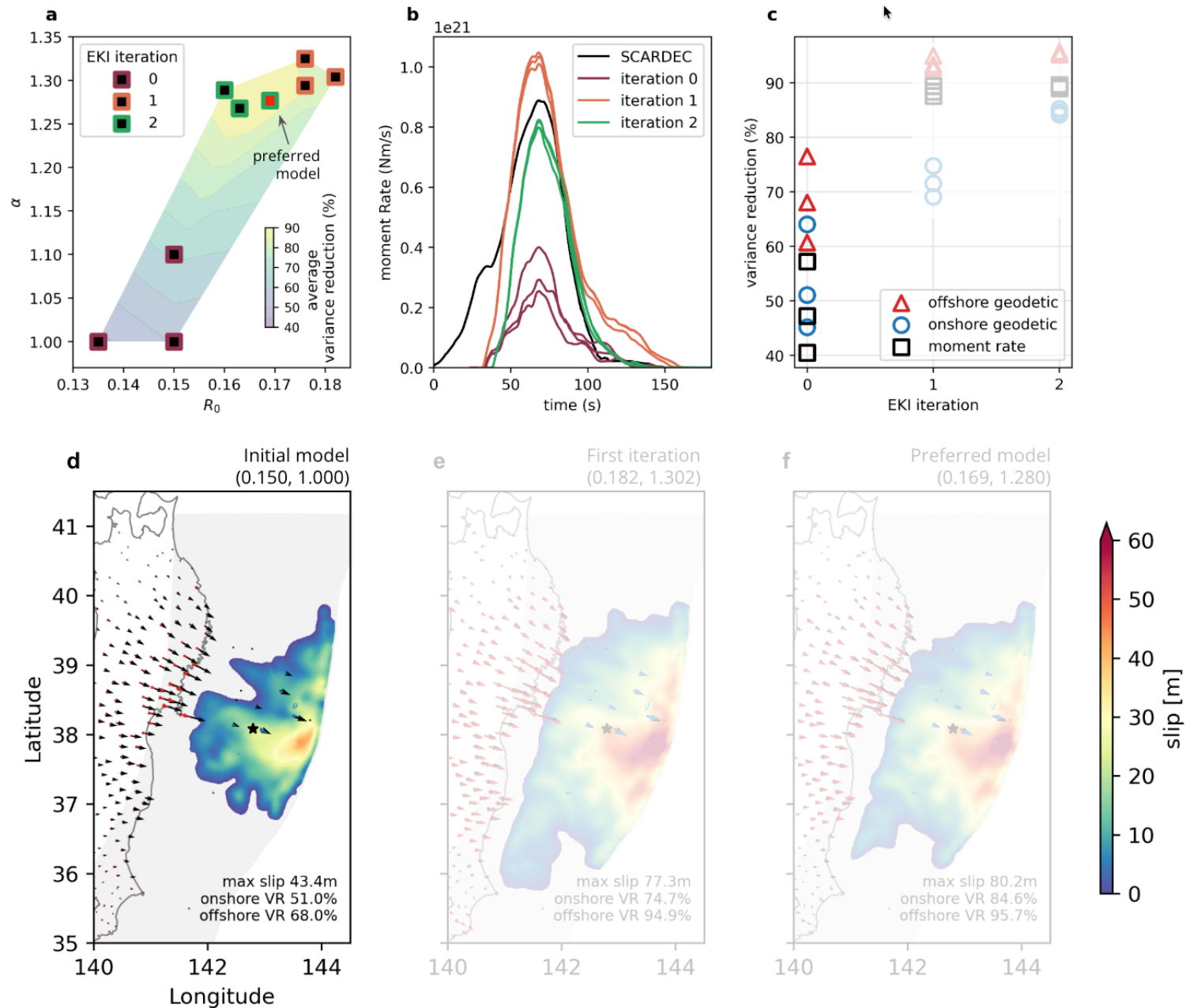
α

R_0

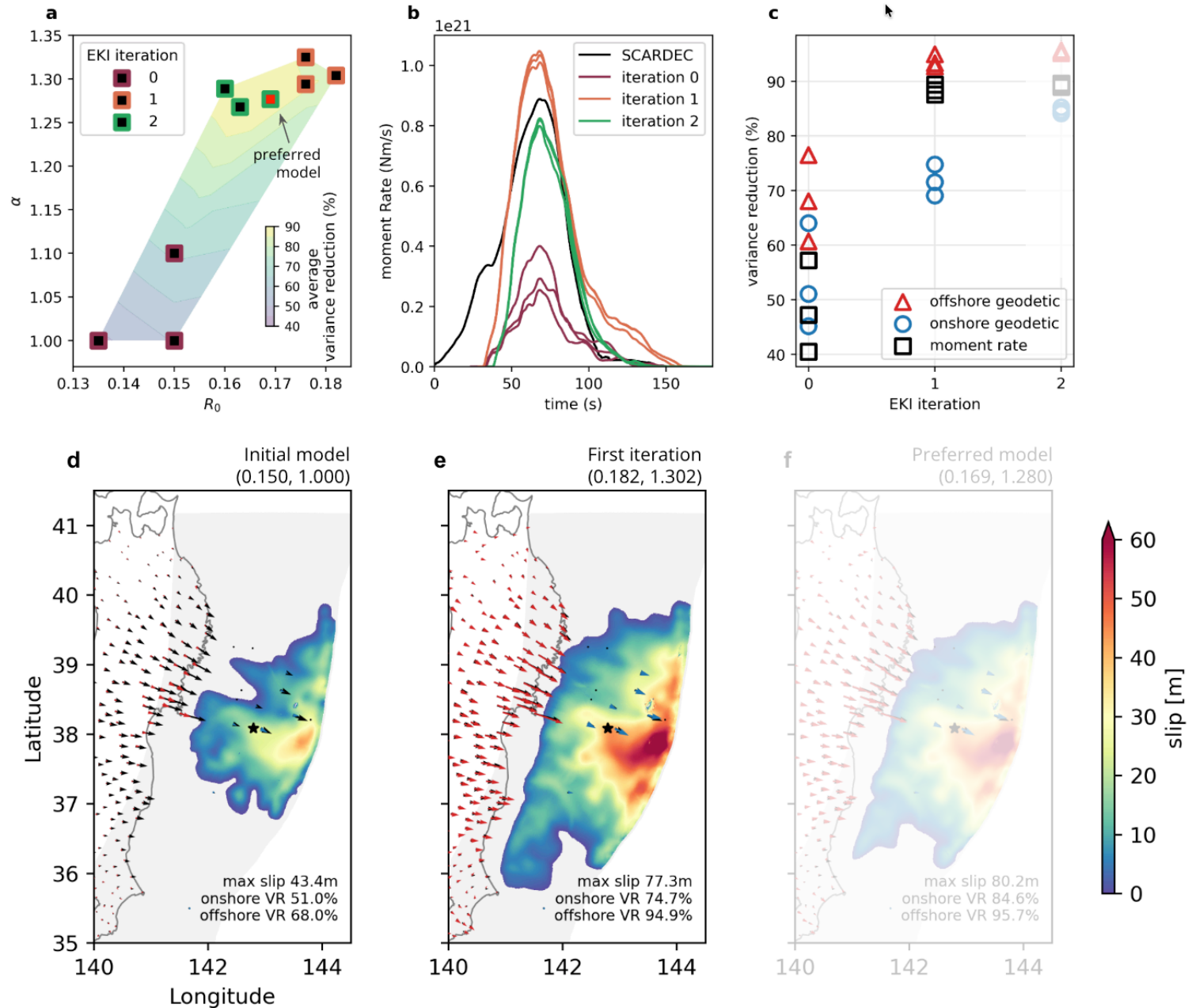
- Compare with onshore and offshore geodetic displacement, moment-rate functions
- Update the ensemble (α, R_0) with EKI



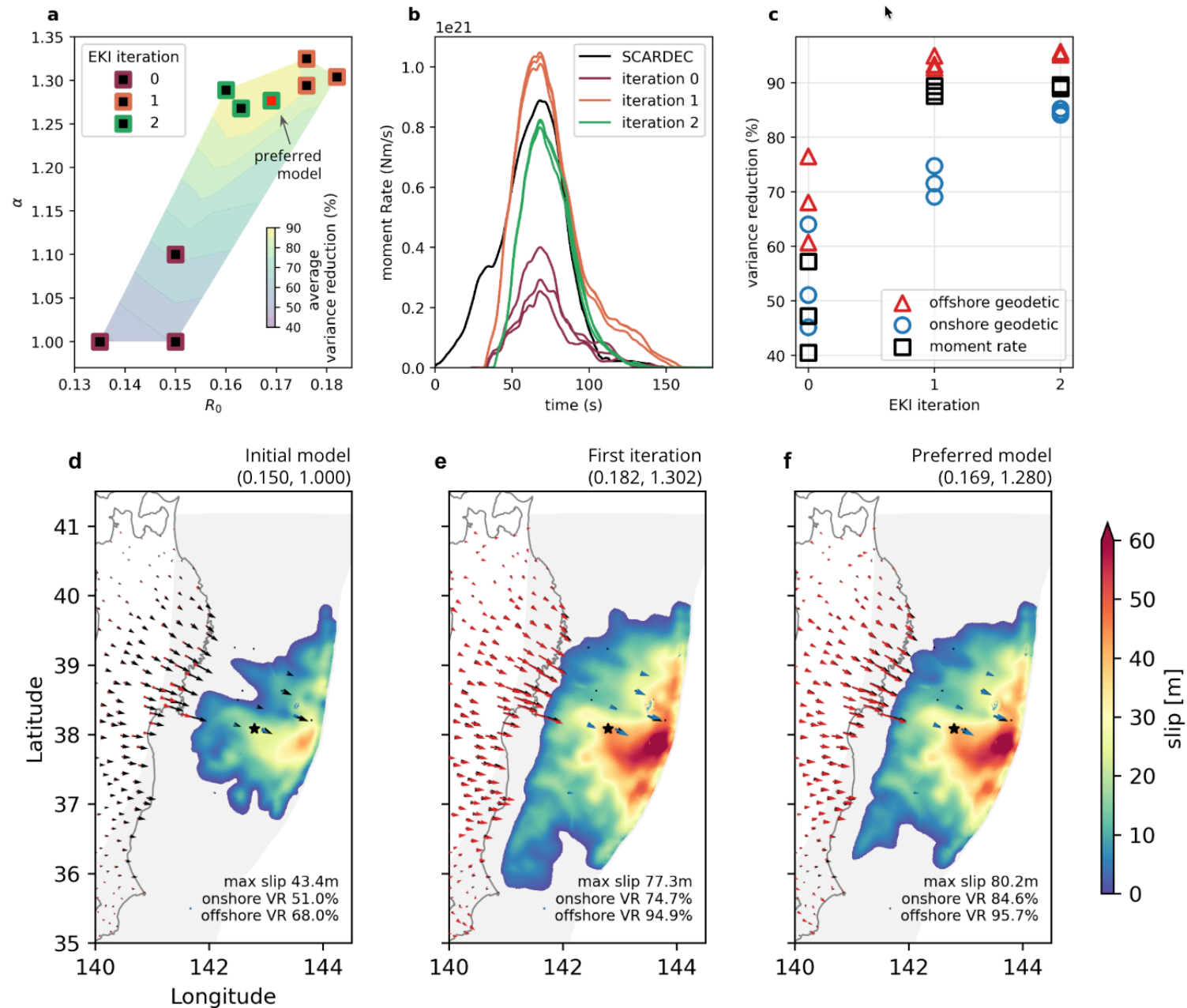
Ensemble Kalman Inversion to identify best-fitting dynamic rupture scenarios



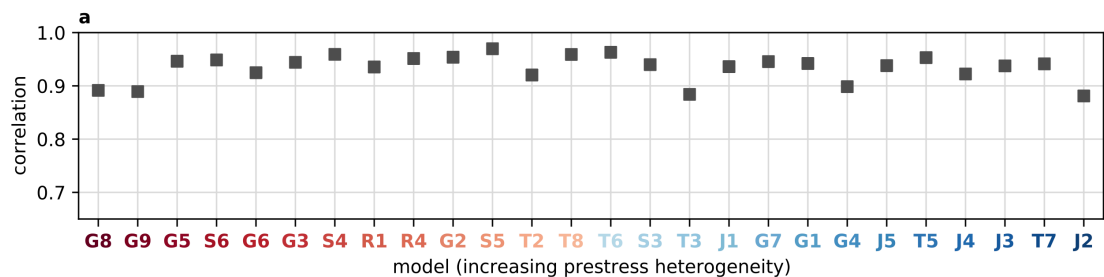
Ensemble Kalman Inversion to identify best-fitting dynamic rupture scenarios



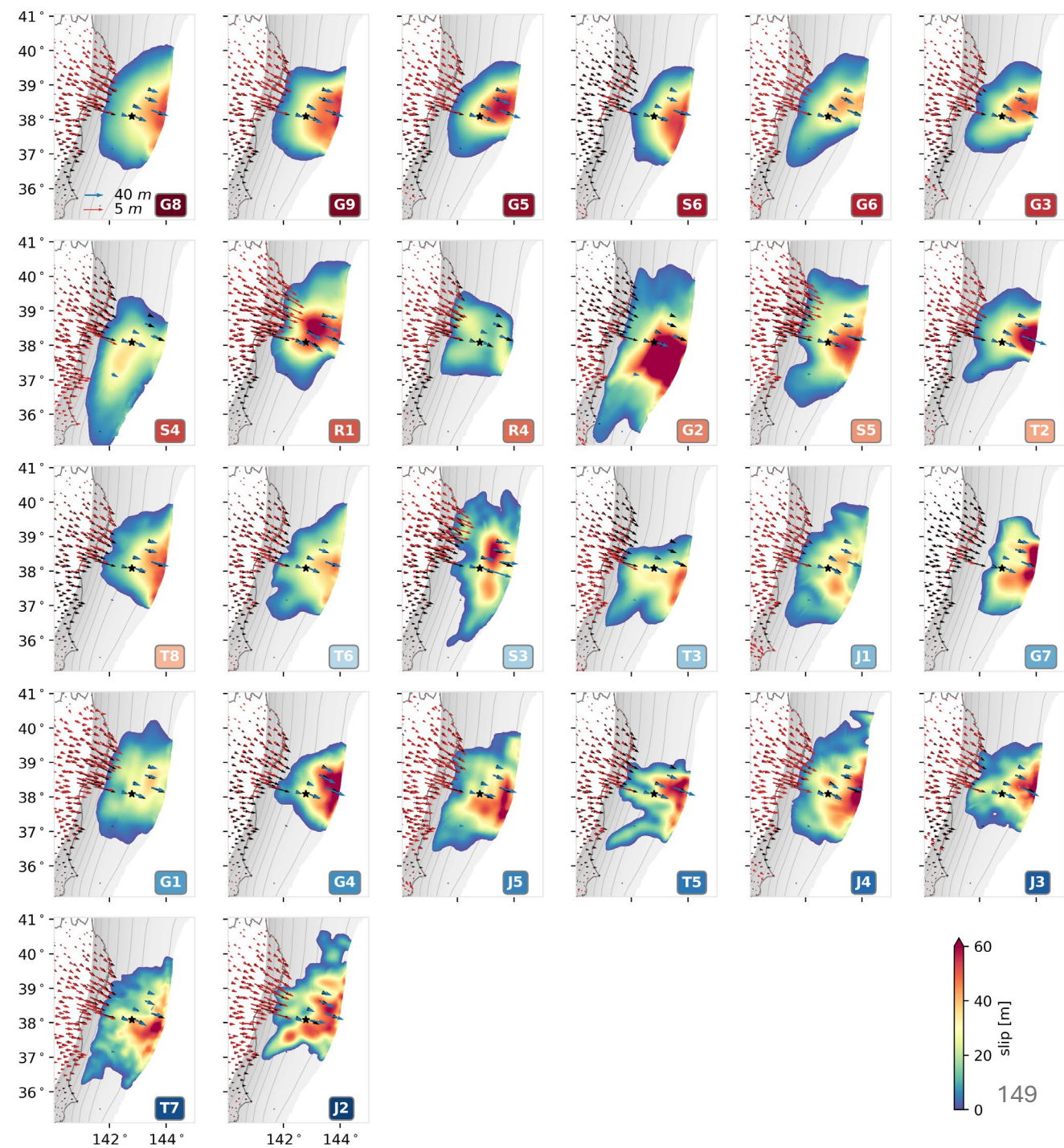
Ensemble Kalman Inversion to identify best-fitting dynamic rupture scenarios



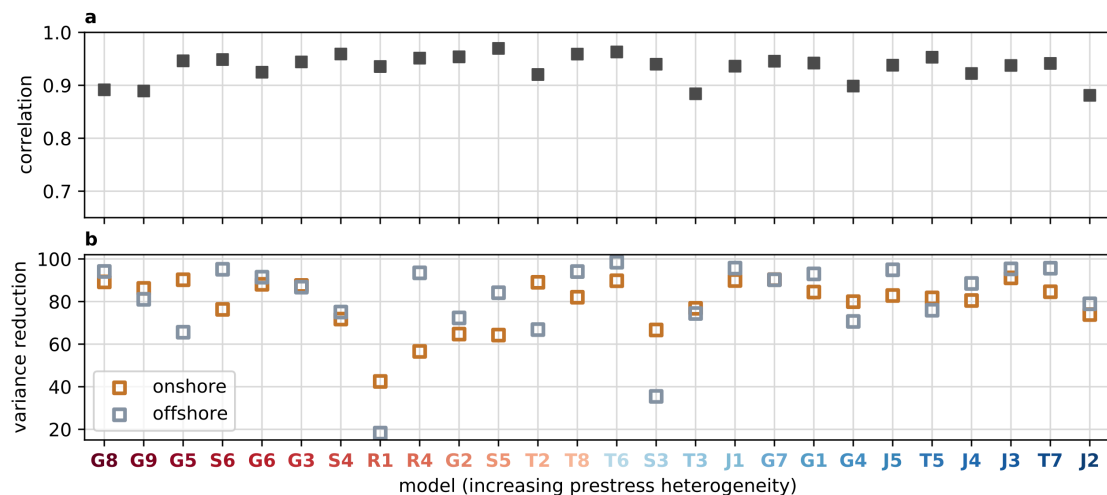
We apply EKI-DR to 32 finite-fault slip models obtain 26 preferred rupture simulations with less than 300 forward simulations in total



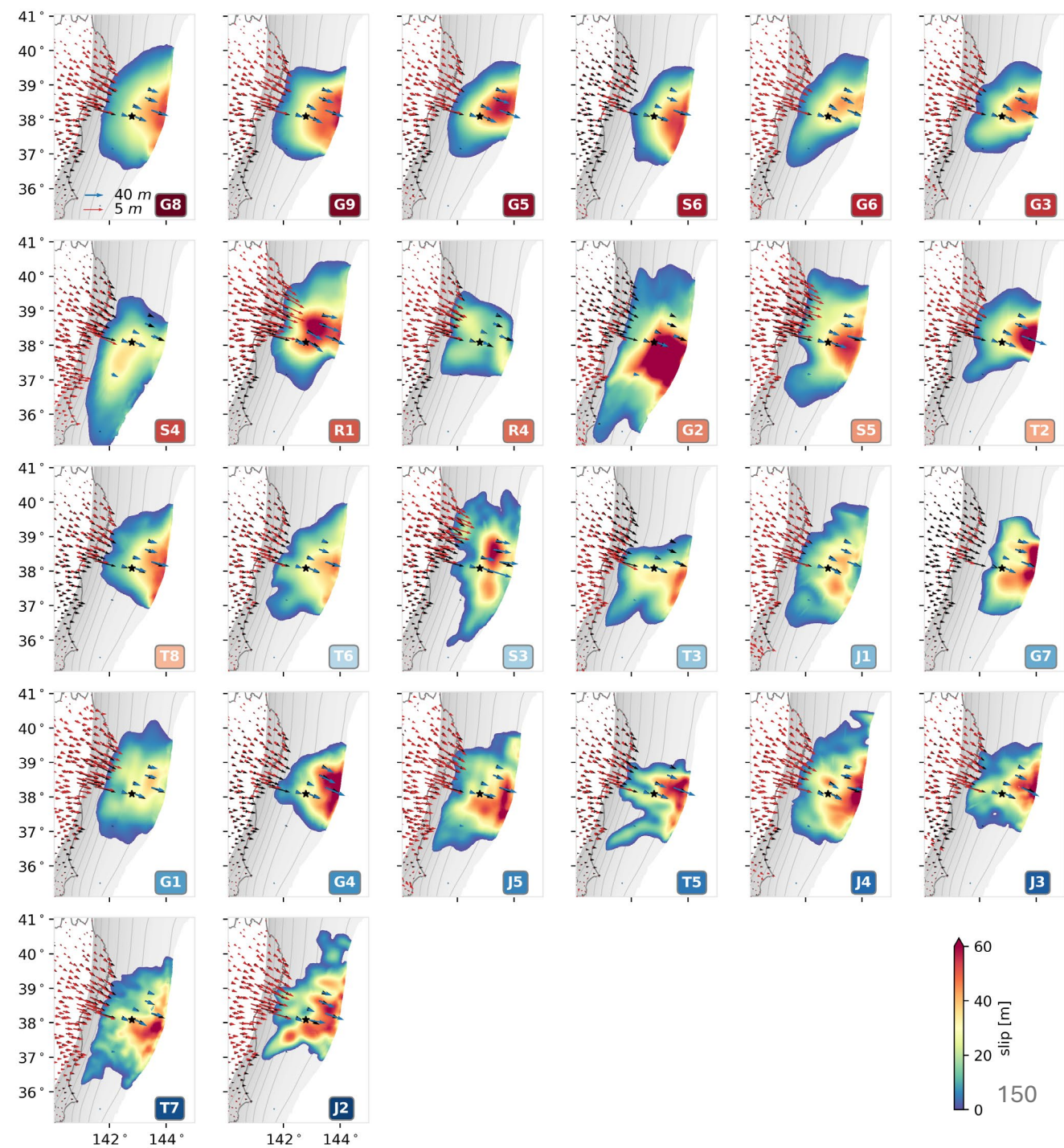
- Contrasting finite-fault slip models can be reproduced dynamically, including both smooth and highly heterogeneous slip distributions



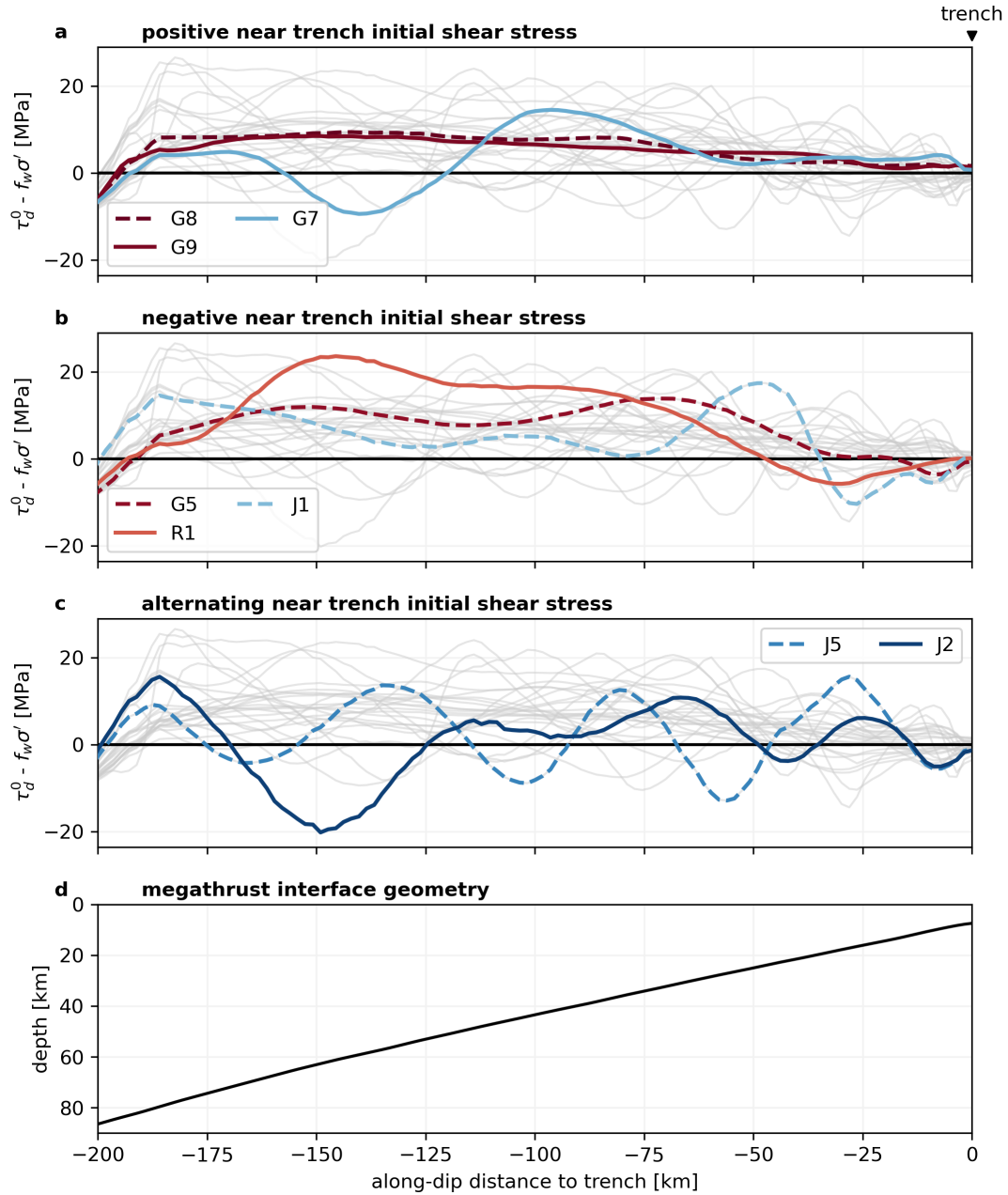
We apply EKI-DR to 32 finite-fault slip models obtain 26 preferred rupture simulations with less than 300 forward simulations in total



- Most rupture models reproduce both onshore and offshore geodetic displacements



Contrasting near-trench initial stress conditions across rupture models



Consistent near-trench slip behavior across rupture models

- DR models show ~10% shallow slip deficit
- 24/26 models suggest trench-breaching slip despite velocity-strengthening friction, limited prestress, and off-fault plastic deformation

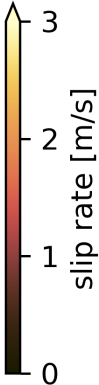
- FFMs show ~50% shallow slip deficit
- Limited trench-slip amplitude

All dynamic rupture models converge to three rupture families

crack-like rupture

single reactivation

multiple reactivation



Smooth prestress distributions promote crack-like rupture

- Circular crack expansion during the first 40 s
- Transition to bilateral rupture after saturating seismogenic width
- Rapid moment release and decay
- Short rupture duration (< 70 s)

Smooth prestress distributions promote single reactivation

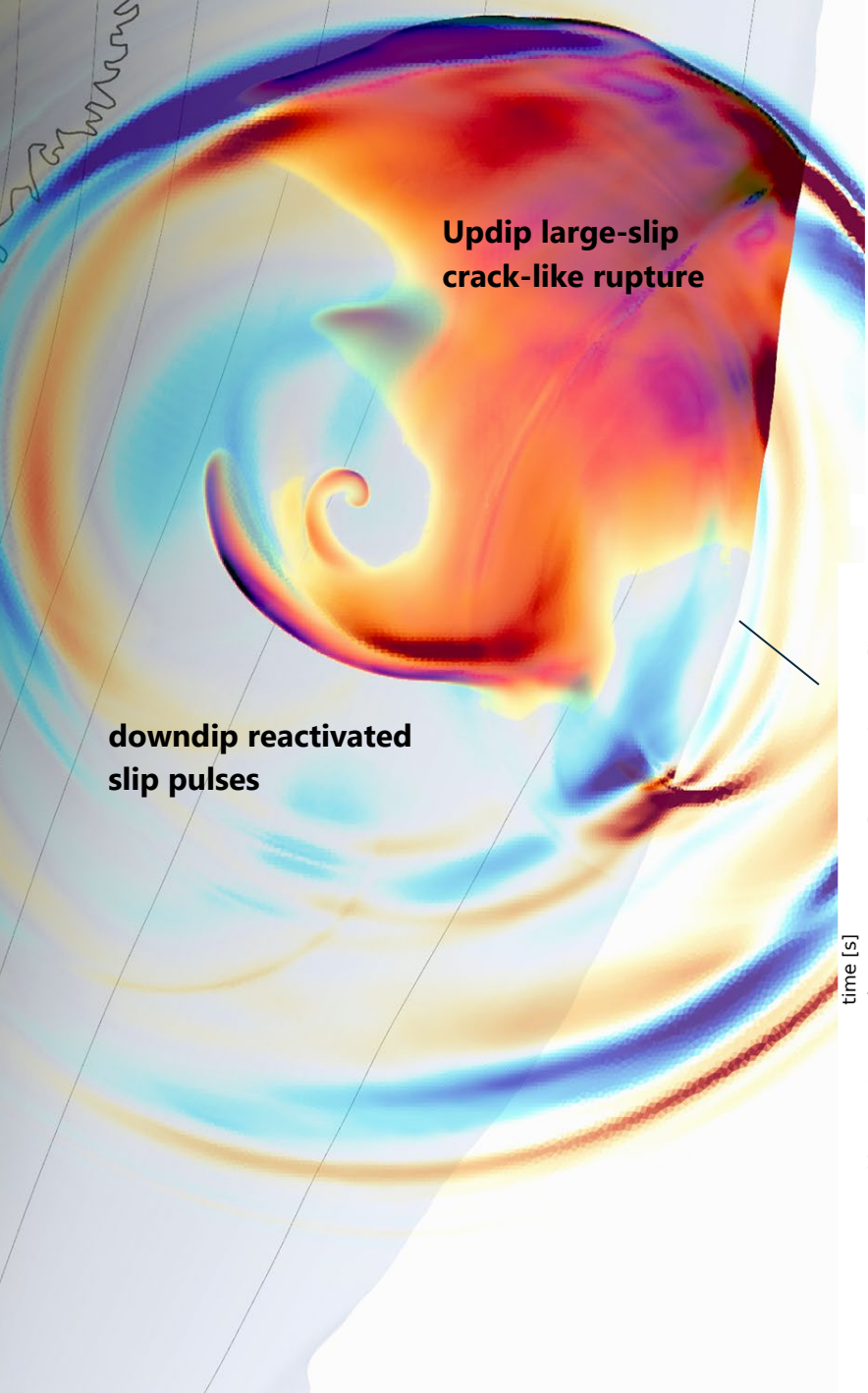
- Single reactivation with pulse-crack transition
- Reactivated front coalescences with the primary front
- Transition to bilateral rupture after saturating seismogenic width
- Distinct two-stage moment-rate release

Heterogeneous prestress distributions promote multiple reactivation

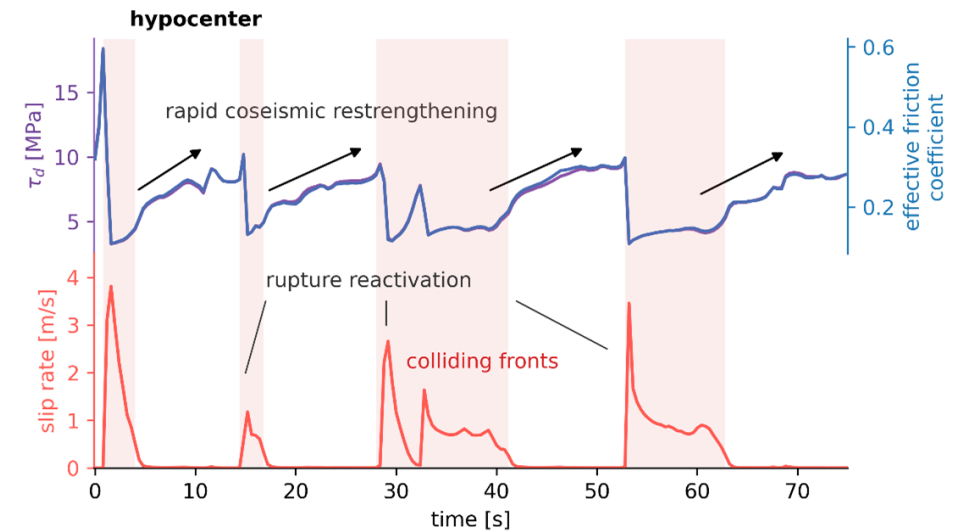
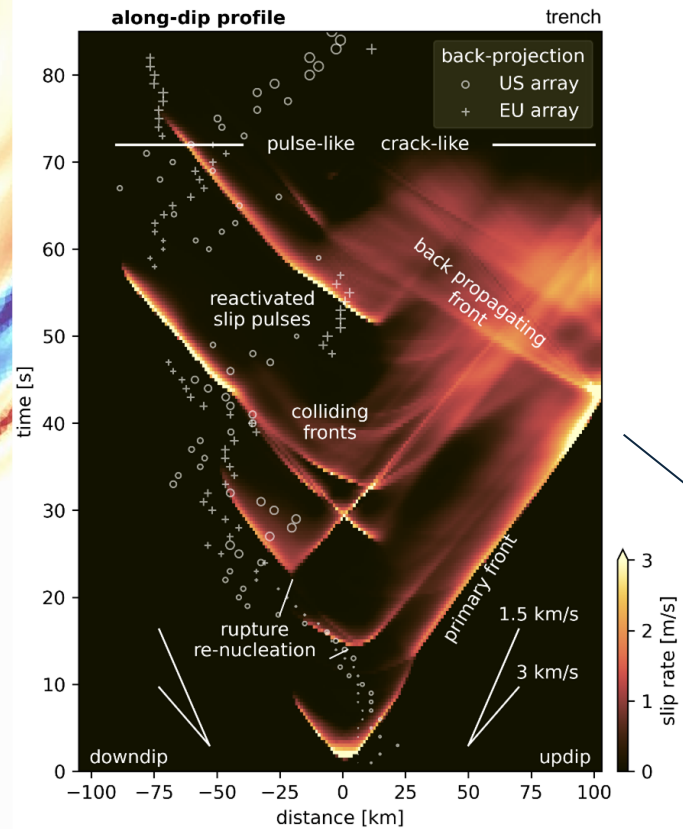
- Depth-dependent rupture behavior
- Up-dip crack-like rupture
- Down-dip reactivated and spiraling slip pulses
- Longer and more complex moment-rate history

Dynamic restrengthening and fault heterogeneity explain megathrust earthquake complexity

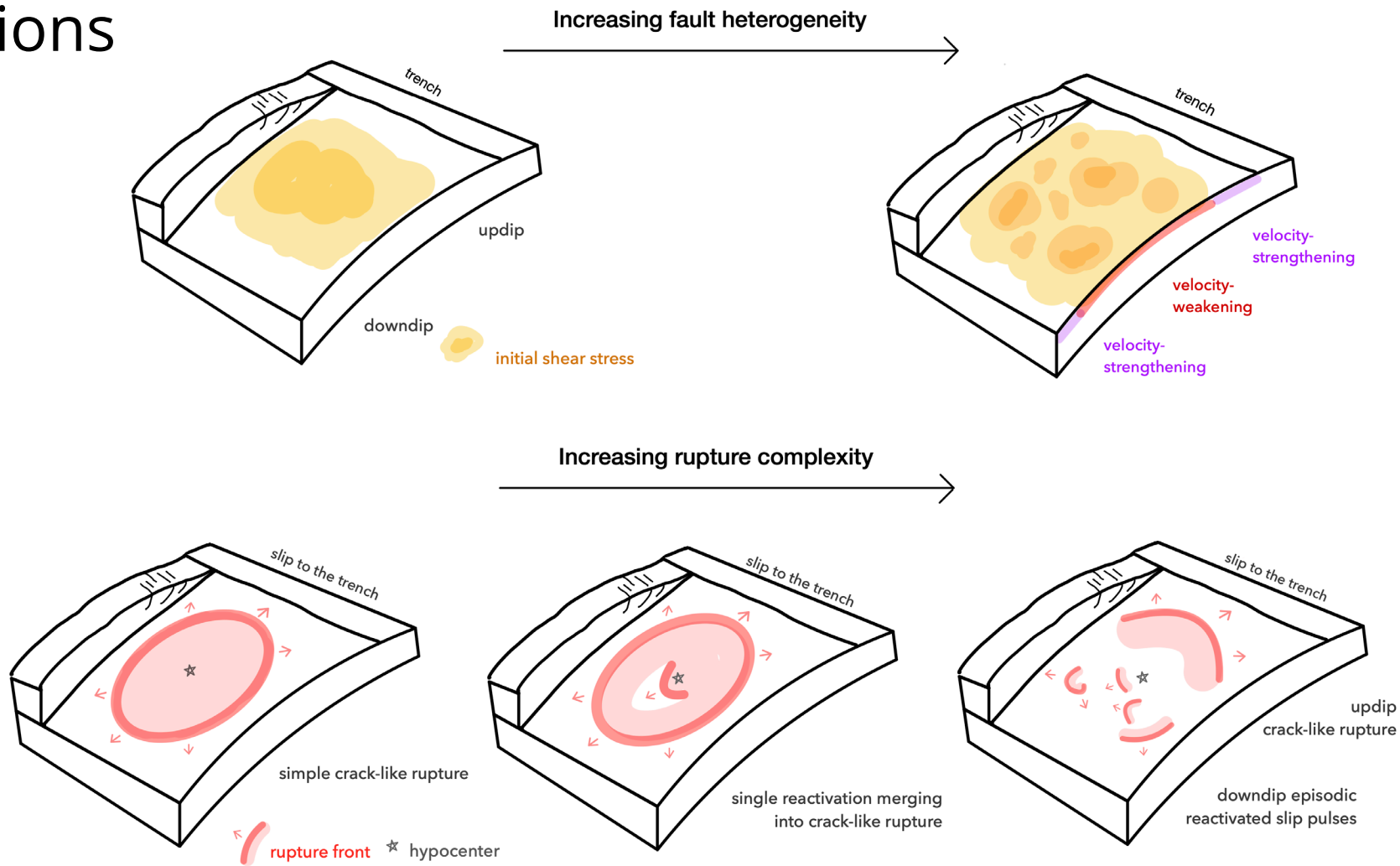
Wong, et al., (2026)



roller coaster of **friction** and **shear stress**



Conclusions



Wong et al., 2024, *JGR: Solid Earth*
Wong et al., 2026, *Nat. Commun.*
Wong et al., in prep

- Ensemble Kalman Inversion (EKI) enables efficient dynamic rupture simulations based on finite-fault slip models
- Using EKI, 26 slip models yield dynamically viable 3D rupture scenarios that match geodetic and teleseismic moment-rate observations
- Contrasting finite-fault slip models converge to **large trench-breaching slip** and **three dynamic model families**, suggesting a few fundamental controls on rupture dynamics